NANO LETTERS

2006
Vol. 6, No. 11
2467−2471

Measuring the Flexibility of Immunoglobulin by Gold Nanoparticles

G. Steven Huang,*,† Yu-Shiun Chen,† and Hsiao-Wei Yeh‡

Institute of Nanotechnology and Center for Nano Science & Technology, National Chiao Tung University, Hsinchu, Taiwan, Republic of China

Received July 12, 2006; Revised Manuscript Received September 14, 2006

ABSTRACT

We measured the flexibility of Fab and Fc arms of immunoglobulin using gold nanoparticles (GNPs). Enzyme-linked immunosorbent assay was performed to measure the affinity of anti-5 nm GNP antiserum against various sizes of GNPs. The flexibility of Fc was also measured by electron microscopy. The restricted binding affinity indicated that only a very limited amount of freedom was allowed for the Fab–Fab hinge, while Fab–Fc showed a much larger degree of freedom.

Immunoglobulin G (IgG) is a Y-shaped molecule composed of two types of fragments: Fab fragments form the two arms, and an Fc fragment forms the stalk of the Y. Crystal structures of intact IgGs—human IgG1, murine IgG1, and murine IgG2a—have been solved by X-ray diffraction analysis.[1−3] Each Fab is connected to an Fc by a flexible hinge of 12−19 amino acids. The hinge allows structural flexibility in the crystal: the Fab arm rotates as much as 158°; the Fab−Fc angle ranges from 66 to 123°; and the Fab−Fab angle ranges from 115 to 172°.[4] Electron microscopy observed up to 180° of rotation for Fab with respect to Fc.[5] Three-dimensional structures of monoclonal IgG determined by cryo-electron tomography show that there is a large degree of freedom for both Fab−Fab hinge and Fab−Fc hinge in solution.[6] This flexibility would allow the IgG molecules a broader range to search for antigens.[7,8] Although the hinges potentially allow fragments to freely move and rotate, it is yet to be determined how this flexibility contributes to antigen recognition.

By convention, proteins of different sizes can serve as a ruler to measure the dynamics of the Fab−Fab angle. This has been demonstrated by analyzing antibody binding to lysozyme, ovalbumin, and bovine serum albumin.[9,10] By measuring the molar ratio of antigen versus antibody, it was concluded that in solution Fab segments present sufficient flexibility that promotes the simultaneous binding of two proteins of 5−9 nm in diameter. Each Fab arm binds one protein independently. In general, binding is facilitated by the flexible and cooperative action of the two Fab arms. When an antibody is immobilized, flexibility is greatly restricted. However, the lack of structural characterization and the comparison of binding between different epitopes restricted generalization of the conclusion.

Applying a biomolecule as an antigen to probe the continuous space for the action of immunoglobulin recognition encountered inevitable problems because the structure of a biomolecule is sequence-specific. Designing a series of biomolecules which continuously change their sizes and at the same time conserve their recognition site is of practical difficulty. Nanoparticles, on the other hand, can be synthesized at desired diameters in the nanometer range. With a uniform surface to serve as an antigen, a spectrum of nanoparticles is potentially a powerful ruler to measure the range of antibody−antigen recognition. The hypothesis underlying the current study was to probe the range of antigen−antibody recognition by applying a broad spectrum of gold nanoparticles (GNPs). The collection of GNPs would thus serve as a molecular ruler to measure the functional flexibility of Fab fragments during the search for antigens.

We synthesized 5, 8, 12, 17, and 37 nm GNPs according to the published procedure.[11,12] Synthesis of GNP was monitored by UV absorbance, and the size was examined by electron microscopy. To obtain antibodies specifically recognizing GNP, BALB/C mice were immunized by weekly intra-peritoneal injection of adjuvant-emulsified 5, 8, 12, 17, and 37 nm GNPs. Mice injected with 8, 12, 17, or 37 nm GNP died within 2 weeks, while mice injected with 5 nm GNP were feeble but survived at the end of the fourth week.

We obtained antiserum from the 5 nm GNP-immunized mice. Enzyme-linked immunosorbent assay (ELISA) was performed to measure the binding activity of anti-5 nm GNP antiserum against 3.5, 4.5, 5, 6, 8, 12, and 17 nm GNP-coated wells (Figure 1).[13] Both control serum and antiserum withdrawn from 12 nm GNP-injected mice (harvested at the second week) showed no reactivity. The anti-5 nm GNP antiserum showed significant binding activity to 3.5, 4.5, 5,

* Corresponding author. E-mail: gstevehuang@mail.nctu.edu.tw.
† Institute of Nanotechnology.
‡ Center for Nano Science & Technology.

10.1021/nl061598x CCC: $33.50 © 2006 American Chemical Society
Published on Web 09/29/2006

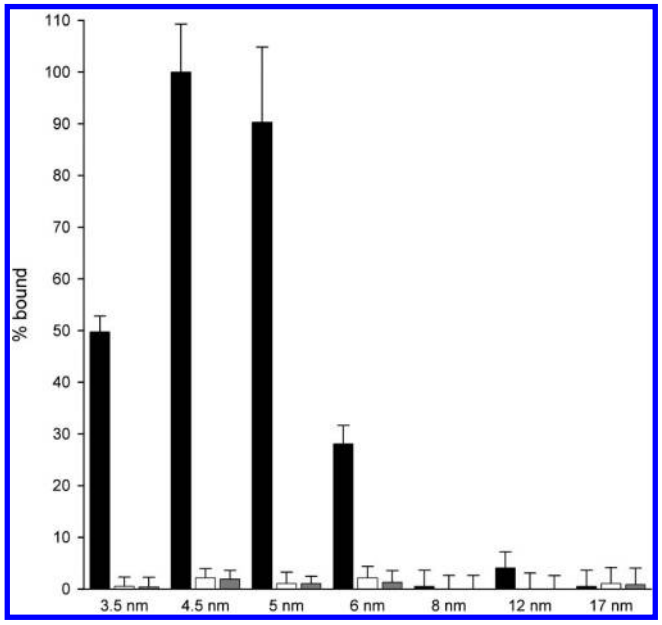

Figure 1. ELISA for anti-5 nm GNP antiserum against gold nanoparticles. Microwells were coated with 3.5, 4.5, 5, 6, 8, 12, and 17 nm GNPs. ELISA was performed using anti-5 nm GNP antiserum (filled bars), normal serum (empty bars), and antiserum withdrawn from 2-week injection of 12 nm GNP mice (gray bars). Anti-5 nm GNP antiserum showed binding activity for 3.5 nm (49.7%), 4.5 nm (100%), 5 nm (90.2%), and 6 nm (28.1%), but no binding activity for GNP larger than 8 nm. Normal serum and antiserum withdrawn from 2-week injection of 12 nm GNP mice showed only background intensity to all GNPs.

and 6 nm GNPs but none to GNPs larger than 8 nm. In particular, the binding activities maximized at 4.5 (100%) and 5 nm (90.2%), dropping to 49.7% for 3.5 nm and to 28.1% for 6 nm GNP.

To examine the specificity of the antibodies binding to the antigen, competition ELISA was performed using GNPs as competitors in preincubation to compete away anti-5 nm GNP binding activity (Figure 2a). The competition ELISA was performed in an Eppendorf tube by adding gradually concentrated competitors to the anti-5 nm gold nanoparticle antiserum in a total volume of 100 μL, incubated 1 h at room temperature, and used as antiserum following the previously described ELISA procedure.[13] Substantial competition activities to the antiserum were observed when 3.5, 4.5, and 5 nm GNPs were applied as competitors. Although 6 nm GNP showed partial binding activity in ELISA, no competing activity was found in the competition assay. Other GNPs showed no competing activity. ZnO nanoparticles of 5 and 20 nm showed no competition (Figure 2b).

The lethal effect of GNP injection is intriguing. The uptake of gold nanoparticles by human cervical cancer cells maximizes for 50 nm GNP.[14] However, GNPs exhibited similar cytotoxicity to mouse fibroblast cells in our cellular survival assay. The injection of GNPs was selectively lethal to mice. Because the survival rate was unrelated to the cytotoxicity of GNPs, the lethality of larger GNPs might be due to the inability of the mouse immune system to generate antibodies that target and scavenge GNPs from circulation.

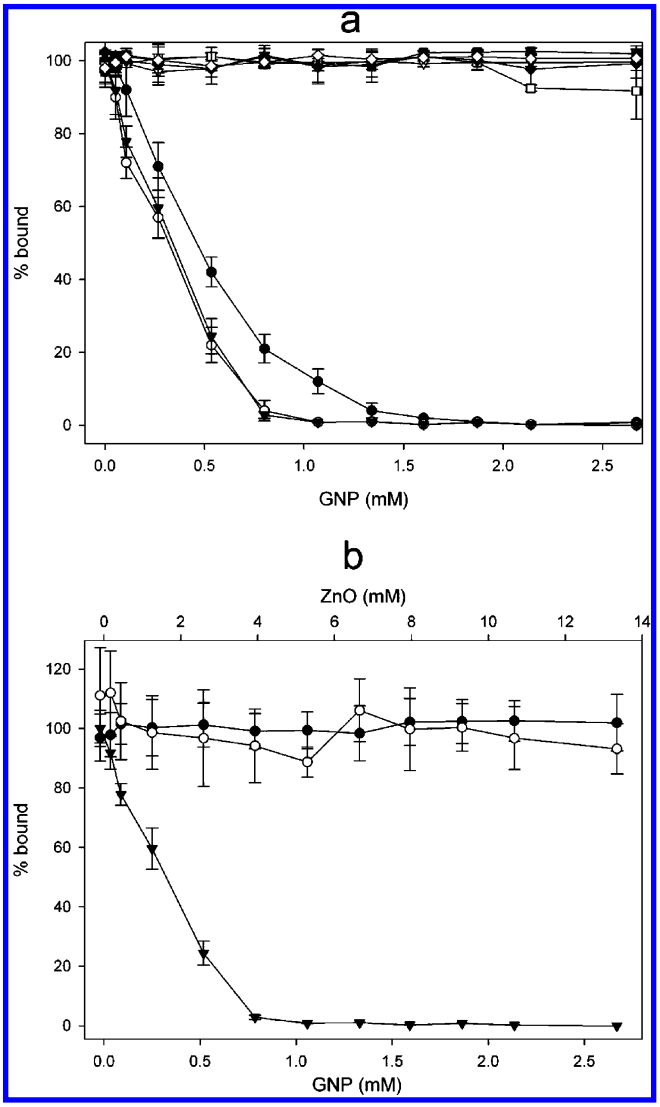

Figure 2. Competition ELISA for the binding of anti-5 nm GNP antiserum and 5 nm GNP. (A) GNPs applied as competitors. GNPs of 3.5 nm (●), 4.5 nm (○), and 5 nm (▼) show substantially competing activities. GNPs of 6 nm (▽), 8 nm (■), 12 nm (□), 17 nm (◆), and 37 nm (◇) fail to affect the binding reaction. (B) 5 nm (●) and 20 nm (○) zinc oxide nanoparticles applied as competitor.

Electron microscopy (EM) imaging might provide structural information of the GNP−immunoglobulin complex (GNP−IgG). To assist visualizing the GNP−IgG complex, we incorporated quantum dots-conjugated goat anti-mouse IgG (QD−IgG) in which a quantum dot (QD) had a defined size of 3 nm and could be unambiguously identified under EM. QD−IgG recognizes the Fc domain of immunoglobulin. The goat anti-mouse IgG-conjugated quantum dots were purified by affinity column before use. Specificity for the Fc fragment was confirmed by ELISA using an Fc fragment as an antigen. The immuno-precipitation of GNP−IgG and QD−IgG was performed, and the precipitate was thoroughly washed, stained with iodine, and examined. The normal serum was co-precipitated with GNP and QD−IgG and served as control. The EM examination was performed using a JEM-2010 electron microscope (JEOL Ltd., Japan) under the specified condition.

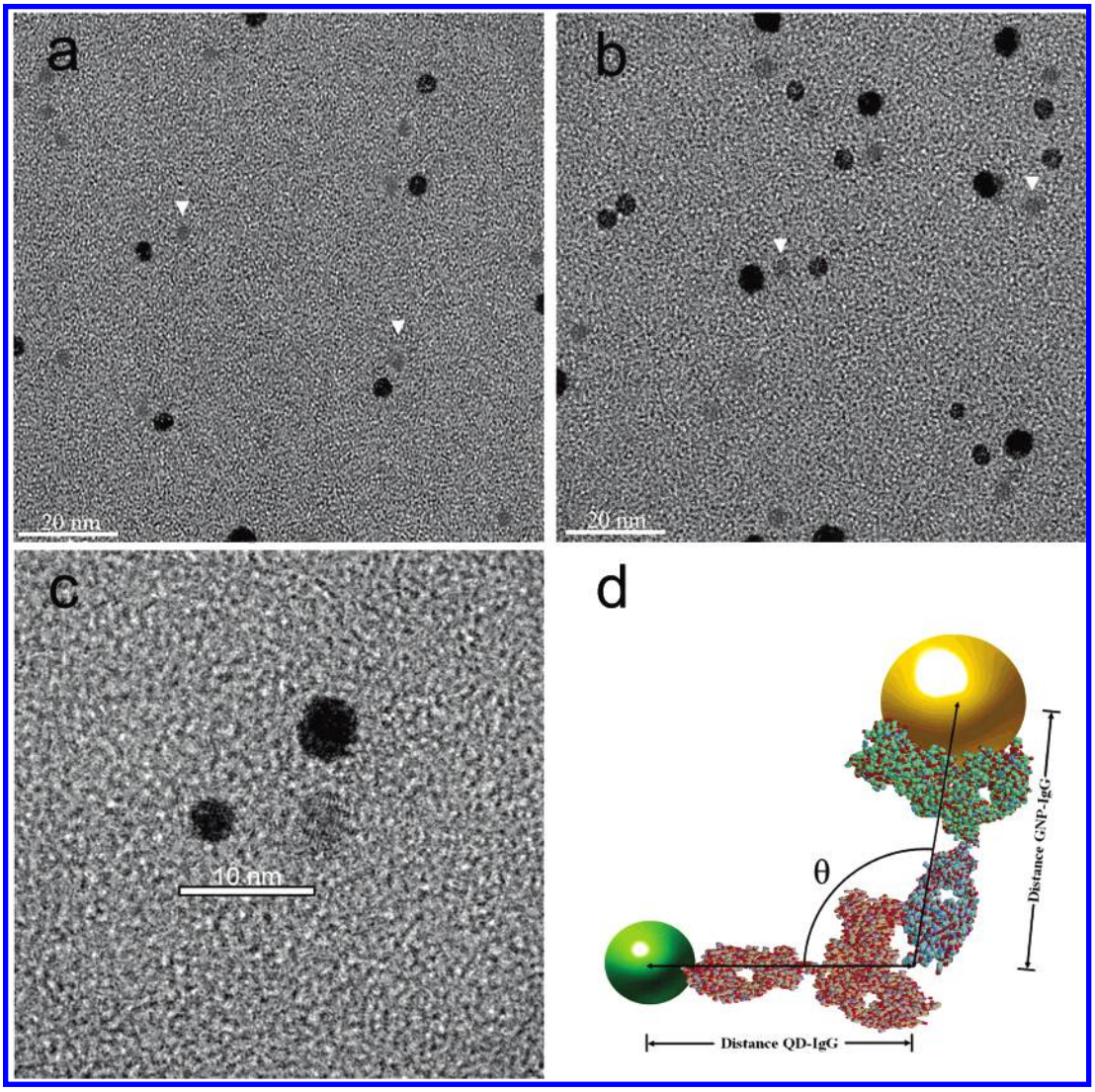

Figure 3. EM image for the co-precipitate of antiserum, 5 nm GNP, and QD−IgG. (A) Control serum is precipitated with 5 nm GNP and quantum dots-conjugated antibody. Most clustered spots are composed of two dots separated by approximately 7 nm. The conformation would fit the described QD−IgG. (B) Anti-5 nm GNP antiserum is precipitated with 5 nm GNP and QD−IgG. A more complex pattern is observed. Each cluster can be dissected into three basic components: 5 nm GNP, 3 nm QD, and IgGs. To assist visualization of protein components, empty triangles are drawn at the top of IgGs. (C) Magnified image from (B) shows a clear GNP−IgGs−QD complex. (D) Molecular model for the GNP−IgGs−QD complex. The molecular model of immunoglobulin is constructed using the crystal structure of IgG2 retrieved from NCBI and with Rasmol graphing software (http://www.umass.edu/microbio/rasmol/).

In the EM images, GNP and QD exhibited solid spheres of 5 and 3 nm, respectively, while protein components showed as a blurred mass (Figure 3). The control experiment exhibited pairwise particles identified as QD−IgG which might have co-precipitated mouse IgG (Figure 3a). Co-precipitation of antiserum, 5 nm GNP, and QD−IgG showed as clusters of three. Each trio was composed of three basic components: a gray protein mass of immunoglobulins, a 5 nm GNP, and a 3 nm QD (Figure 3b). Higher magnification displayed a GNP−IgGs−QD conformation (Figure 3c).

The EM image represented sampling for the conformational space of GNP−(IgGs)−QD complexes. The distances and angles of the triangles were not identical to the distances and angles expected from a crystal structure. It is likely that the GNP−IgGs−QD complex may not lie at a right angle relative to the incoming electron beam; thus, the apparent angles and distances were distorted by tilt angles. To obtain the GNP−(IgGs)−QD angle, a ball-and-stick model was proposed (Figure 3d). Assuming the GNP−(IgGs)−QD triangle with a top angle θ_0 sitting with a tilt angle ω against the horizontal plane (Figure 4), the apparent top angle (θ), the apparent distance of GNP−IgG (A), and the apparent distance of QD−IgG (B) can be described as functions of tilt angle (ω):

$$\theta = \pi - \tan^{-1}\left(\frac{H_0 \cos\omega}{L_1}\right) - \tan^{-1}\left(\frac{H_0 \cos\omega}{L_2}\right) \quad (1)$$

$$\theta_0 = \cos^{-1}\left(\frac{H_0}{A_0}\right) + \cos^{-1}\left(\frac{H_0}{B_0}\right) \quad (2)$$

$$A = \sqrt{A_0^2 - H_0^2(1 - \cos^2\omega)} \quad (3)$$

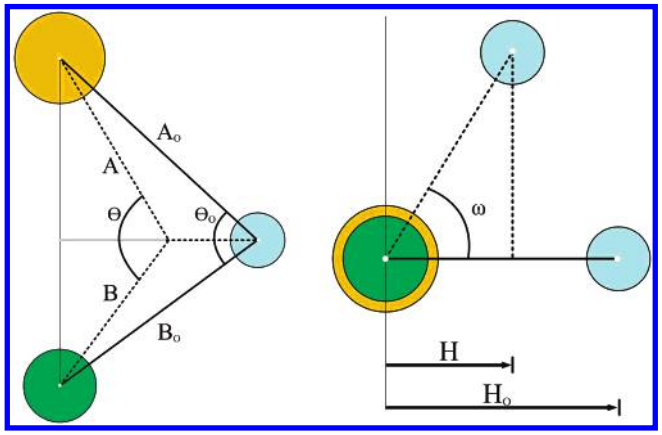

Figure 4. Schematic drawing for ball-and-stick model. The drawing shows top view (left) and side view (right) for the GNP−(IgGs)−QD triangle with a top angle θ_0 sitting at a tilt angle ω against the horizontal plane. Yellow circle represents 5 nm GNP. Green circle represents 3 nm QD. In the drawing, θ is the apparent top angle; A_0 is the distance of GNP−IgG (8.5 nm); A is the apparent distance of GNP−IgG; B_0 is the distance of QD−IgG (7.7 nm); B is the apparent distance of QD−IgG; H is the apparent height of the triangle; and H_0 is the height of the triangle.

$$B = \sqrt{B_0^2 - H_0^2(1 - \cos^2 \omega)} \tag{4}$$

$$L_1 = \sqrt{A_0^2 - H_0^2} \tag{5}$$

$$L_2 = \sqrt{B_0^2 - H_0^2} \tag{6}$$

where A_0 is the distance of GNP−IgG (8.5 nm); A is the apparent distance of GNP−IgG; B_0 is the distance of QD−IgG (7.7 nm); B is the apparent distance of QD−IgG; and H_0 is the height of the triangle.

Each θ_0 describes a hyperbolic line in three-dimensional space (Figure 5) using A, B, and θ as axes. These hyperbolic lines of various θ_0 collectively form a plane. To assign θ_0 for each complex, A, B, and θ were measured from image and plotted in 3D space. The GNP−IgGs−QD complexes were spotted from EM images primarily by the sizes of GNP (5 nm) and QD (3 nm). Energy dispersive X-ray analysis (EDX) was performed to identify the composition of Au and Cd. Complexes meeting these two criteria were selected for distance and angle analysis as shown in Figure 5. Thirty-four complexes were chosen from 54 candidates. Deviation of the experimental points away from the plane was observed, probably due to the heterogeneous nature of polyclonal antibodies used in this study, or due to minor denaturation occurring to protein components during the processing of specimens. The theoretical θ_0 was obtained by projecting each point onto the θ_0 plane (Figure 6). The acquired θ_0 was distributed between 35 and 120° and maximized at 100°. It was then realized that the flexibility of θ_0 is shared by two Fab−Fc hinges: anti-GNP IgG and QD-conjugated IgG (Figure 3d). Furthermore, the observed θ_0 might not reflect the actual bending of the two hinges due to the blurriness of the EM images. Nevertheless, the GNP−IgGs−QD complex exhibited comparable flexibility as previously reported for Fab−Fc hinges.[7,8]

Because all GNPs have identical surfaces to serve as an epitope for anti-GNP immunoglobulin, the free rotation and movement of Fab arms would allow binding of GNP as large as 17 nm.[10] The inability of antiserum to recognize GNPs larger than 5 nm indicated that the range of antigen recognition is restricted. Factors other than the flexibility of Fab arms must be involved. While the size of GNP increased, the local conformation of the recognition site on immunoglobulin would have to gradually change to adapt the changing geometry of antigens. Since the local conformation of the binding site is determined by amino acid sequence, the restricted structural adaptation might cause failure in antigen recognition for larger GNPs. On the other hand, the Fc−Fc hinges were found to be highly flexible in that two hinges collectively presented 85° of freedom in the GNP−IgGs−QD complex.

This letter provided a novel platform to measure the functional flexibility of immunoglobulin. The structural information was attained with biochemical and EM images without complicated or tedious procedures.

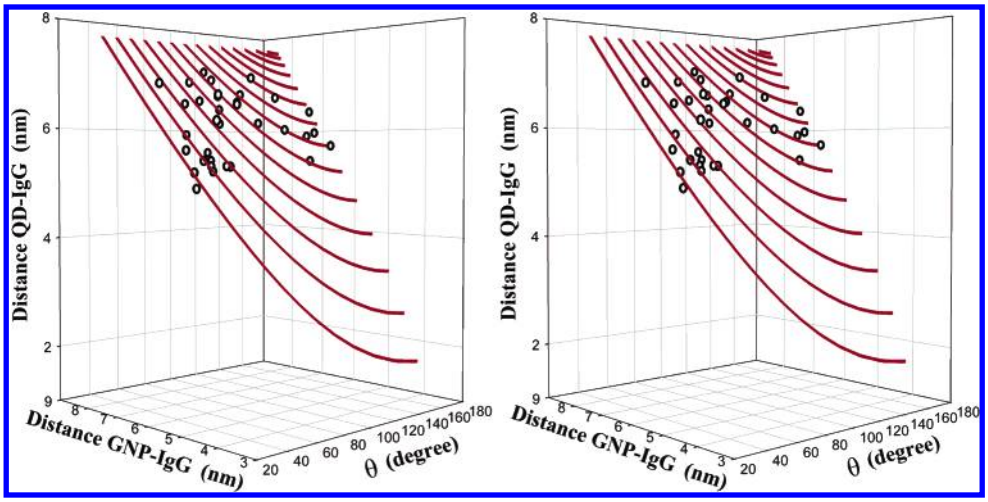

Figure 5. Stereoview of 3D plots for the measured angle and distances of GNP−IgGs−QD complexes obtained from cryo-EM. Each hyperbolic line represents simulated angle and distances for a specific θ_0. Collection of θ_0 from 35 to 180° forms a plane in 3D space.

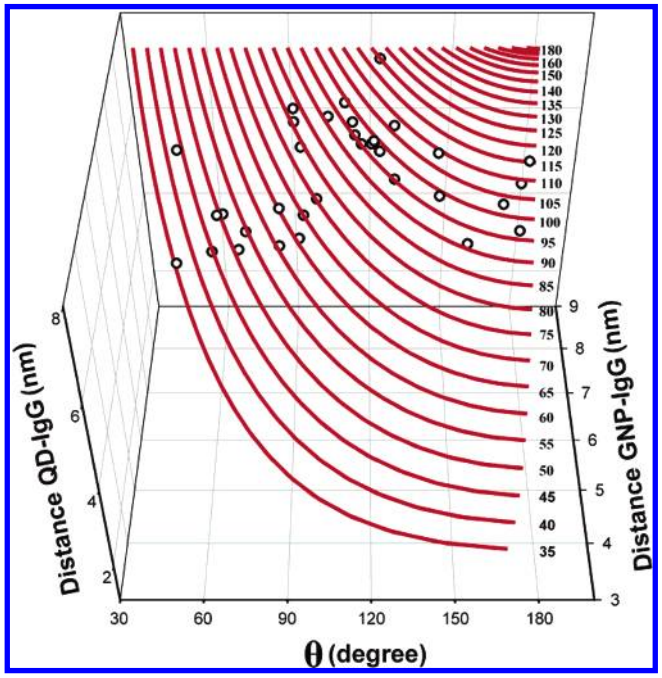

Figure 6. Projection of apparent angle and distances of GNP−IgGs−QD complexes onto the theoretical θ_0 plane. Three-dimensional plot is adjusted to a view perpendicular to the theoretical θ_0 plane. Each point falls on the plane and is assigned to a corresponding θ_0.

Acknowledgment. This study was supported in part by National Science Council Grant NSC94-2320-B-009-003 and Bureau of Animal and Plant Health Inspection and Quarantine Council of Agriculture Grants 95AS-13.3.1-BQ-B1 and 95AS-13.3.1-BQ-B6.

References

(1) Harris, L. J.; Larson, S. B.; Hasel, K. W.; Day, J.; Greenwood, A.; McPherson, A. *Nature* **1992**, *360*, 369.
(2) Harris, L. J.; Skaletsky, E.; McPherson, A.; Larson, S. B.; Hasel, K. W.; Day, J.; Greenwood, A. *J. Mol. Biol.* **1998**, *275*, 861.
(3) Saphire, E. O.; Parren, P. W.; Pantophlet, R.; Zwick, M. B.; Morris, G. M.; Rudd, P. M.; Dwek, R. A.; Stanfield, R. L.; Burton, D. R.; Wilson, I. A. *Science* **2001**, *293*, 1155.
(4) Saphire, E. O.; Stanfield, R. L.; Crispin, M. D.; Parren, P. W.; Rudd, P. M.; Dwek, R. A.; Burton, D. R.; Wilson, I. A. *J. Mol. Biol.* **2002**, *319*, 9.
(5) Wade, R. H.; Taveau, J. C.; Lamy, J. N. *J. Mol. Biol.* **1989**, *206*, 349.
(6) Sandin, S.; Ofverstedt, L. G.; Wikstrom, A. C.; Wrange, O.; Skoglund, U. *Structure* **2004**, *12*, 409.
(7) Smith, T. J.; Olson, N. H.; Cheng, R. H.; Chase, E. S.; Baker, T. S. *Proc. Natl. Acad. Sci. U.S.A.* **1993**, *90*, 7015.
(8) Roux, K. H.; Strelets, L.; Michaelsen, T. E. *J. Immunol.* **1997**, *159*, 3372.
(9) Oda, M.; Azuma, T. *Mol. Immunol.* **2000**, *37*, 1111.
(10) Oda, M.; Uchiyama, S.; Robinson, C. V.; Fukui, K.; Kobayashi, Y.; Azuma, T. *FEBS J.* **2006**, *273*, 1476.
(11) Brown, K. R.; Walter, D. G.; Natan, M. J. *Chem. Mater.* **2000**, *12*, 306.
(12) Liu, F.-K.; Ker, C.-J.; Chang, Y.-C.; Ko, F.-H.; Chu, T.-C.; Dai, B.-T. *Jpn. J. Appl. Phys.* **2003**, *42*, 4152.
(13) Engvall, E.; Pearlmann, P. *Immunochemistry* **1971**, *8*, 871.
(14) Chithrani, B. D.; Ghazani, A. A.; Chan, W. C. *Nano Lett.* **2006**, *6*, 662.

NL061598X